

Observation of $B^+ \rightarrow K_1(1270)^+ \gamma$

Heyoung Yang,³⁶ M. Nakao,⁸ K. Abe,⁸ K. Abe,⁴¹ H. Aihara,⁴³ Y. Asano,⁴⁷ T. Aushev,¹² S. Bahinipati,⁴ A. M. Bakich,³⁸ Y. Ban,³² I. Bedny,¹ U. Bitenc,¹³ I. Bizjak,¹³ S. Blyth,²⁵ A. Bondar,¹ A. Bozek,²⁶ M. Bračko,^{8,19,13} J. Brodzicka,²⁶ T. E. Browder,⁷ M.-C. Chang,²⁵ P. Chang,²⁵ Y. Chao,²⁵ A. Chen,²³ W. T. Chen,²³ B. G. Cheon,³ R. Chistov,¹² S.-K. Choi,⁶ Y. Choi,³⁷ Y. K. Choi,³⁷ A. Chuvikov,³³ S. Cole,³⁸ J. Dalseno,²⁰ M. Dash,⁴⁸ S. Eidelman,¹ Y. Enari,²¹ F. Fang,⁷ N. Gabyshev,¹ A. Garmash,³³ T. Gershon,⁸ G. Gokhroo,³⁹ B. Golob,^{18,13} J. Haba,⁸ K. Hayasaka,²¹ H. Hayashii,²² M. Hazumi,⁸ L. Hinz,¹⁷ T. Hokuue,²¹ Y. Hoshi,⁴¹ Y. B. Hsiung,²⁵ T. Iijima,²¹ A. Imoto,²² K. Inami,²¹ Y. Iwasaki,⁸ J. H. Kang,⁴⁹ J. S. Kang,¹⁵ S. U. Kataoka,²² N. Katayama,⁸ H. Kawai,² T. Kawasaki,²⁸ H. R. Khan,⁴⁴ H. Kichimi,⁸ H. J. Kim,¹⁶ J. H. Kim,³⁷ S. K. Kim,³⁶ S. M. Kim,³⁷ T. H. Kim,⁴⁹ K. Kinoshita,⁴ S. Korpar,^{19,13} P. Krokovny,¹ C. C. Kuo,²³ A. Kuzmin,¹ Y.-J. Kwon,⁴⁹ J. S. Lange,⁵ G. Leder,¹¹ S. H. Lee,³⁶ T. Lesiak,²⁶ J. Li,³⁵ S.-W. Lin,²⁵ G. Majumder,³⁹ T. Matsumoto,⁴⁵ A. Matyja,²⁶ W. Mitaroff,¹¹ K. Miyabayashi,²² H. Miyake,³⁰ H. Miyata,²⁸ R. Mizuk,¹² T. Nagamine,⁴² Y. Nagasaka,⁹ E. Nakano,²⁹ Z. Natkaniec,²⁶ S. Nishida,⁸ O. Nitoh,⁴⁶ S. Ogawa,⁴⁰ T. Ohshima,²¹ T. Okabe,²¹ S. Okuno,¹⁴ S. L. Olsen,⁷ W. Ostrowicz,²⁶ P. Pakhlov,¹² H. Palka,²⁶ C. W. Park,³⁷ N. Parslow,³⁸ R. Pestotnik,¹³ L. E. Piilonen,⁴⁸ M. Rozanska,²⁶ H. Sagawa,⁸ Y. Sakai,⁸ N. Sato,²¹ T. Schietinger,¹⁷ O. Schneider,¹⁷ J. Schümann,²⁵ C. Schwanda,¹¹ A. J. Schwartz,⁴ R. Seuster,⁷ H. Shibuya,⁴⁰ A. Somov,⁴ N. Soni,³¹ R. Stamen,⁸ S. Stanič,^{47,*} M. Starič,¹³ K. Sumisawa,³⁰ T. Sumiyoshi,⁴⁵ S. Suzuki,³⁴ S. Y. Suzuki,⁸ O. Tajima,⁸ F. Takasaki,⁸ N. Tamura,²⁸ M. Tanaka,⁸ G. N. Taylor,²⁰ Y. Teramoto,²⁹ X. C. Tian,³² T. Tsukamoto,⁸ S. Uehara,⁸ T. Uglov,¹² K. Ueno,²⁵ S. Uno,⁸ Y. Ushiroda,⁸ G. Varner,⁷ K. E. Varvell,³⁸ S. Villa,¹⁷ C. H. Wang,²⁴ M.-Z. Wang,²⁵ M. Watanabe,²⁸ A. Yamaguchi,⁴² Y. Yamashita,²⁷ M. Yamauchi,⁸ Y. Yuan,¹⁰ L. M. Zhang,³⁵ Z. P. Zhang,³⁵ V. Zhilich,¹ D. Žontar,^{18,13} and D. Zürcher¹⁷

(Belle Collaboration)

¹*Budker Institute of Nuclear Physics, Novosibirsk*²*Chiba University, Chiba*³*Chonnam National University, Kwangju*⁴*University of Cincinnati, Cincinnati, Ohio 45221*⁵*University of Frankfurt, Frankfurt*⁶*Gyeongsang National University, Chinju*⁷*University of Hawaii, Honolulu, Hawaii 96822*⁸*High Energy Accelerator Research Organization (KEK), Tsukuba*⁹*Hiroshima Institute of Technology, Hiroshima*¹⁰*Institute of High Energy Physics, Chinese Academy of Sciences, Beijing*¹¹*Institute of High Energy Physics, Vienna*¹²*Institute for Theoretical and Experimental Physics, Moscow*¹³*J. Stefan Institute, Ljubljana*¹⁴*Kanagawa University, Yokohama*¹⁵*Korea University, Seoul*¹⁶*Kyungpook National University, Taegu*¹⁷*Swiss Federal Institute of Technology of Lausanne, EPFL, Lausanne*¹⁸*University of Ljubljana, Ljubljana*¹⁹*University of Maribor, Maribor*²⁰*University of Melbourne, Victoria*²¹*Nagoya University, Nagoya*²²*Nara Women's University, Nara*²³*National Central University, Chung-li*²⁴*National United University, Miao Li*²⁵*Department of Physics, National Taiwan University, Taipei*²⁶*H. Niewodniczanski Institute of Nuclear Physics, Krakow*²⁷*Nihon Dental College, Niigata*²⁸*Niigata University, Niigata*²⁹*Osaka City University, Osaka*³⁰*Osaka University, Osaka*³¹*Panjab University, Chandigarh*³²*Peking University, Beijing*³³*Princeton University, Princeton, New Jersey 08545*

- ³⁴Saga University, Saga
³⁵University of Science and Technology of China, Hefei
³⁶Seoul National University, Seoul
³⁷Sungkyunkwan University, Suwon
³⁸University of Sydney, Sydney NSW
³⁹Tata Institute of Fundamental Research, Bombay
⁴⁰Toho University, Funabashi
⁴¹Tohoku Gakuin University, Tagajo
⁴²Tohoku University, Sendai
⁴³Department of Physics, University of Tokyo, Tokyo
⁴⁴Tokyo Institute of Technology, Tokyo
⁴⁵Tokyo Metropolitan University, Tokyo
⁴⁶Tokyo University of Agriculture and Technology, Tokyo
⁴⁷University of Tsukuba, Tsukuba
⁴⁸Virginia Polytechnic Institute and State University, Blacksburg, Virginia 24061
⁴⁹Yonsei University, Seoul

(Received 12 December 2004; published 24 March 2005)

We report the observation of the radiative decay $B^+ \rightarrow K_1(1270)^+ \gamma$ using a data sample of 140 fb^{-1} taken at the $\Upsilon(4S)$ resonance with the Belle detector at the KEKB e^+e^- collider. We find the branching fraction to be $\mathcal{B}(B^+ \rightarrow K_1(1270)^+ \gamma) = (4.3 \pm 0.9(\text{stat.}) \pm 0.9(\text{syst.})) \times 10^{-5}$ with a significance of 7.3σ . We find no significant signal for $B^+ \rightarrow K_1(1400)^+ \gamma$ and set an upper limit $\mathcal{B}(B^+ \rightarrow K_1(1400)^+ \gamma) < 1.5 \times 10^{-5}$ at the 90% confidence level. We also measure inclusive branching fractions for $B^+ \rightarrow K^+ \pi^+ \pi^- \gamma$ and $B^0 \rightarrow K^0 \pi^+ \pi^- \gamma$ in the mass range $1 \text{ GeV}/c^2 < M_{K^{+(0)}\pi^+\pi^-} < 2 \text{ GeV}/c^2$.

DOI: 10.1103/PhysRevLett.94.111802

PACS numbers: 13.20.He, 14.40.Nd

Radiative B decays that occur through the flavor changing neutral current process $b \rightarrow s\gamma$ have been one of the most sensitive probes in the search for physics beyond the standard model (SM). The first observed exclusive radiative decay mode was $B \rightarrow K^* \gamma$ [1,2]. The second mode was $B \rightarrow K_2^*(1430)\gamma$, for which evidence was reported by CLEO and Belle [1]. Theoretical predictions for the branching fractions of the unobserved exclusive decays can be found in Refs. [3,4]. The modes $B \rightarrow K_1(1270)\gamma$ and $B \rightarrow K_1(1400)\gamma$ ($K_1 \rightarrow K\pi\pi$) can be used to measure the photon helicity, which may differ from the SM prediction in some models beyond the SM [5]. The neutral mode $B^0 \rightarrow K_1(1270)^0\gamma$, $K_1(1270)^0 \rightarrow K_S^0\rho^0$ would also be useful to measure time-dependent CP violation that may arise from new physics [6].

In this Letter, we report the observation of $B^+ \rightarrow K_1(1270)^+ \gamma$, which is the first radiative B meson decay mode that involves an axial-vector resonance. We study radiative decays in the $K^+ \pi^+ \pi^- \gamma$ and $K_S^0 \pi^+ \pi^- \gamma$ final states, where we search for resonant structure in the $K\pi^+\pi^-$ system [7]. We also report inclusive measurements of $B^+ \rightarrow K^+ \pi^+ \pi^- \gamma$ and $B^0 \rightarrow K^0 \pi^+ \pi^- \gamma$, and the results of a search for $B^+ \rightarrow K_1(1400)^+ \gamma$. The analysis is based on a data sample of 140 fb^{-1} ($152 \times 10^6 \text{ } B\bar{B}$ pairs) taken at the $\Upsilon(4S)$ resonance with the Belle detector at the KEKB e^+e^- collider [8].

The Belle detector consists of a three-layer silicon vertex detector (SVD), a 50-layer central drift chamber (CDC), an array of aerogel threshold Čerenkov counters (ACC), a barrel-like arrangement of time-of-flight scintillation

counters (TOF), and an electromagnetic calorimeter comprised of CsI(Tl) crystals (ECL) located inside a superconducting solenoid coil that provides a 1.5 T magnetic field. An instrumented iron flux-return (KLM) for K_L^0 and muon identification is located outside of the coil. The detector is described in detail elsewhere [9].

The photon candidate is the highest energy photon cluster measured with the barrel ECL ($33^\circ < \theta_\gamma < 128^\circ$ in the laboratory frame). In order to reduce the background from $\pi^0/\eta \rightarrow \gamma\gamma$ decays, we combine the photon candidate with all other photon clusters in the event with energy greater than 30 MeV (200 MeV) and reject the event if the invariant mass of any pair is within $\pm 18 \text{ MeV}/c^2$ ($\pm 32 \text{ MeV}/c^2$) of the nominal π^0 (η) mass. These correspond to $\pm 3\sigma$ windows, where σ is the mass resolution. We refer to this requirement as the π^0/η veto.

Charged tracks are required to have momentum in the center-of-mass (c.m.) frame greater than $200 \text{ MeV}/c$ and to have an impact parameter relative to the interaction point of less than 5 cm along the positron beam axis and less than 0.5 cm in the transverse plane. The charged kaon candidate is identified using a likelihood ratio combining the information from the ACC, TOF, and CDC subdetectors; the remaining charged particles in the event are used as pion candidates, unless the track has been identified as an electron, muon, or proton.

For neutral kaons, we use $K_S^0 \rightarrow \pi^+\pi^-$ candidates that have invariant masses within $\pm 30 \text{ MeV}/c^2$ of the nominal K_S^0 mass and a c.m. momentum greater than $200 \text{ MeV}/c$. The two pions are required to have a common vertex that is

displaced from the interaction point. The K_S^0 momentum direction is also required to be consistent with the K_S^0 flight direction.

In order to study $B \rightarrow K_1 \gamma$ ($K_1 \rightarrow K \pi \pi$), we first reconstruct $B \rightarrow K \pi^+ \pi^- \gamma$ inclusively, without any requirement for the structure of the $K \pi^+ \pi^-$ system. We select $K \pi^+ \pi^-$ combinations in the mass range $1 \text{ GeV}/c^2 < M_{K \pi^+ \pi^-} < 2 \text{ GeV}/c^2$. Given the $K \pi^+ \pi^-$ system and the photon candidate, we identify B meson candidates using two independent kinematic variables: the beam-energy constrained mass $M_{bc} \equiv \sqrt{(E_{\text{beam}}^*/c^2)^2 - |\vec{p}_B^*/c|^2}$ and the energy difference $\Delta E \equiv E_{K \pi \pi}^* + E_\gamma^* - E_{\text{beam}}^*$, where E_{beam}^* is the beam energy and \vec{p}_B^* is the momentum of the B candidate in the c.m. frame [10]. The B momentum is calculated as $\vec{p}_B^* = \vec{p}_{K \pi \pi}^* + \frac{\vec{p}_\gamma^*}{E_\gamma^*} \times (E_{\text{beam}}^* - E_{K \pi \pi}^*)$ in order to improve the M_{bc} resolution. We select B candidates within $-0.1 \text{ GeV} < \Delta E < 0.08 \text{ GeV}$ and $M_{bc} > 5.2 \text{ GeV}/c^2$. If there exist multiple candidates, we choose the candidate with the highest confidence level for the $K^+ \pi^+ \pi^-$ vertex fit ($\pi^+ \pi^-$ vertex in the neutral case).

The dominant background comes from hadronic continuum ($e^+ e^- \rightarrow q \bar{q}$, $q = u, d, s, c$). To suppress this background, we use two variables: the B flight direction ($\cos \theta_B^*$) and a Fisher discriminant [11] built from a set of shape variables [12]. For signal, the B flight direction follows a $1 - \cos^2 \theta_B^*$ distribution while that of $q \bar{q}$ is nearly uniform. The likelihood function $\mathcal{L}_{S(B)}^{\cos \theta_B^*}$ is modeled as a second (first) order polynomial for the signal (continuum background) from Monte Carlo (MC) samples. For the shape variables, we use 16 modified Fox-Wolfram moments [13] calculated for the following groups of particles: (1) particles that form the signal candidate, (2) the remaining charged particles, (3) the remaining neutral particles, and (4) a hypothetical particle for the missing momentum of the event. The Fisher discriminant is obtained from these moments and the scalar sum of the transverse momentum. The likelihood function $\mathcal{L}_{S(B)}^{\text{Fisher}}$ is modeled as a bifurcated Gaussian function both for the signal and the continuum background from MC samples.

These likelihood functions are then combined to form $\mathcal{R}_S = \mathcal{L}_S^{\cos \theta_B^*} \mathcal{L}_S^{\text{Fisher}} / (\mathcal{L}_S^{\cos \theta_B^*} \mathcal{L}_S^{\text{Fisher}} + \mathcal{L}_B^{\cos \theta_B^*} \mathcal{L}_B^{\text{Fisher}})$. We determine the \mathcal{R}_S requirement by maximizing $N_S / \sqrt{N_S + N_B}$, where N_S and N_B are the expected number of the signal and background events, respectively, in $M_{bc} > 5.27 \text{ GeV}/c^2$. For this purpose, we use $B \rightarrow K_1(1270) \gamma$ and $B \rightarrow K_1(1400) \gamma$ signal MC simulated data, assuming all the $B \rightarrow K_1 \gamma$ branching fractions are 1×10^{-5} . We find $\mathcal{R}_S > 0.9$ is the optimal requirement. This requirement retains 47% of the signal events while rejecting 98% of the continuum background events.

The signal yields for $B \rightarrow K \pi^+ \pi^- \gamma$ are extracted from a binned maximum likelihood fit to the M_{bc} distribution. In addition to the continuum background, we consider four B

decay background sources: known B decays through the $b \rightarrow c$ transition (referred to as the $b \rightarrow c$ background), hadronic B decays through the $b \rightarrow u, d, \text{ or } s$ transitions (charmless background), $B \rightarrow K^* \gamma$ background, and radiative $b \rightarrow s$ decays to final states other than $K^* \gamma$ and $K \pi^+ \pi^- \gamma$ (other $b \rightarrow s \gamma$ background). To suppress the $B \rightarrow K^* \gamma$ background, we reject the event if ΔE and M_{bc} calculated from either $K \pi \gamma$ combination satisfy $-0.2 \text{ GeV} < \Delta E < 0.1 \text{ GeV}$ and $M_{bc} > 5.27 \text{ GeV}/c^2$. The signal M_{bc} distributions are each modeled as a Gaussian function; its width is fixed using a data sample of $B \rightarrow D(\rightarrow K \pi \pi) \pi$ decays, treating the primary pion as a high energy photon. The shapes of the background M_{bc} distributions are determined using large MC samples. We find that the sum of the continuum and $b \rightarrow c$ backgrounds is described by an ARGUS function [14], a smooth functional form that has a kinematic threshold at half of the center-of-mass energy. Charmless decays, $B \rightarrow K^* \gamma$, and other $b \rightarrow s \gamma$ decays are modeled as a sum of an ARGUS function and a Gaussian function. The normalization of the continuum plus $b \rightarrow c$ background is floated in the fit; the normalization of the other three components are fixed in the fit.

The fit result is shown in Fig. 1. For the $B^+ \rightarrow K^+ \pi^+ \pi^- \gamma$ mode, we obtain 318 ± 22 events with a significance of 16σ , where the significance is defined as $\sqrt{-2 \ln(\mathcal{L}_0/\mathcal{L}_{\text{max}})}$, and \mathcal{L}_{max} and \mathcal{L}_0 denote the maximum likelihoods of the fit with and without the signal component, respectively, and the significance includes systematic error. Similarly, we obtain 67 ± 10 events with a significance of 8.3σ for the $B^0 \rightarrow K^0 \pi^+ \pi^- \gamma$ mode.

The systematic uncertainty related to the fitting procedure is estimated in the following way. We vary the width and the mean of the signal Gaussian by the error of the $B \rightarrow D \pi$ calibration sample. We vary the ARGUS parameter of the continuum plus $b \rightarrow c$ background by the errors from fits to the MC sample and to a data sideband region defined as $0.1 \text{ GeV} < \Delta E < 0.5 \text{ GeV}$, then we take the quadratic sum of those errors. The $B \rightarrow K^* \gamma$ component is varied by the branching fraction uncertainty. The normalization of the other $b \rightarrow s \gamma$ background component is varied within

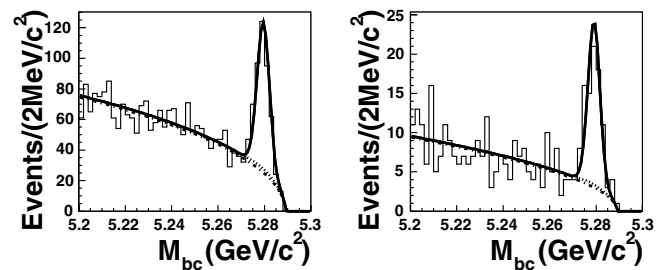


FIG. 1. M_{bc} distributions for $B^+ \rightarrow K^+ \pi^+ \pi^- \gamma$ (left) and $B^0 \rightarrow K^0 \pi^+ \pi^- \gamma$ (right). Curves show the continuum plus $b \rightarrow c$ background component (dot-dashed), total background (dotted), and the total fit result (solid).

its respective uncertainty, estimated from the uncertainties in the total $b \rightarrow s\gamma$ branching fraction [15] and the fraction of $K\pi^+\pi^-\gamma$ in the $s\gamma$ final state [16]. For the charmless background we vary the normalization by $\pm 100\%$. We also assign the uncertainty due to a possible fit bias as the error of the fit to the signal MC sample. The total fitting errors are 5.3% (12%) for the $B^+ \rightarrow K^+\pi^+\pi^-\gamma$ ($B^0 \rightarrow K^0\pi^+\pi^-\gamma$) mode.

In order to decompose intermediate resonances that may be involved in the $K^+\pi^+\pi^-$ final state, we perform an unbinned maximum likelihood fit to the M_{bc} and $M_{K^+\pi^+\pi^-}$ distributions of the $B^+ \rightarrow K^+\pi^+\pi^-\gamma$ candidates. There are many possible resonances that can contribute: $K_1(1270)$, $K_1(1400)$, $K_2^*(1430)$, $K^*(1410)$, $K^*(1680)$, and so on. We consider the first three resonances, and include an additional nonresonant $B^+ \rightarrow K^+\pi^+\pi^-\gamma$ component. The $B \rightarrow K_2^*(1430)\gamma$ component, which is already measured, is fixed in the fit. We model the $M_{K^+\pi^+\pi^-}$ distribution of the $K_1(1270)$ resonance as a sum of three decay chains, $K_1(1270)^+ \rightarrow K^+\rho^0$, $\rho^0 \rightarrow \pi^+\pi^-$; $K_1(1270)^+ \rightarrow K^{*0}\pi^+$, $K^{*0} \rightarrow K^+\pi^-$; and $K_1(1270)^+ \rightarrow K_0^*(1430)^0\pi^+$, $K_0^*(1430)^0 \rightarrow K^+\pi^-$. The $M_{K^+\pi^+\pi^-}$ distribution for each decay chain is described by convolving the two relativistic Breit-Wigner functions of the resonances in the decay chain. The $M_{K^+\pi^+\pi^-}$ distribution of the $K_1(1400)$ resonance is modeled with a single decay chain, $K_1(1400)^+ \rightarrow K^{*0}\pi^+$, $K^{*0} \rightarrow K^+\pi^-$. The $M_{K^+\pi^+\pi^-}$ distributions of other $b \rightarrow s\gamma$, nonresonant $B^+ \rightarrow K^+\pi^+\pi^-\gamma$, and continuum plus $b \rightarrow c$ backgrounds are modeled using the function $(p_0 + p_1x)\exp(p_2 + p_3x + p_4x^2)$, where $x = M_{K^+\pi^+\pi^-}$, and p_i ($i = 0 \dots 4$) are empirical parameters that are determined from MC samples.

In order to enhance the $K_1(1270)$ component, we select events with $\pi^+\pi^-$ mass in the ρ^0 mass region, $0.6 \text{ GeV}/c^2 < M_{\pi\pi} < 0.9 \text{ GeV}/c^2$ [$\mathcal{B}(K_1(1270) \rightarrow K\rho) = (42 \pm 6)\%$ being much larger than $\mathcal{B}(K_1(1400) \rightarrow K\rho) =$

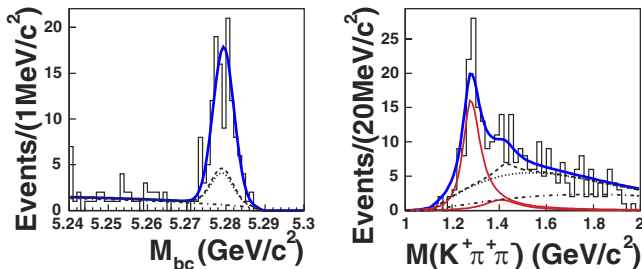


FIG. 2 (color online). M_{bc} distribution for $1.2 \text{ GeV}/c^2 < M_{K^+\pi^+\pi^-} < 1.4 \text{ GeV}/c^2$ (left) and $M_{K^+\pi^+\pi^-}$ distribution for $M_{bc} > 5.27 \text{ GeV}/c^2$ (right) of the $K_1(1270)^+\gamma$ enriched sample with $0.6 \text{ GeV}/c^2 < M_{\pi\pi} < 0.9 \text{ GeV}/c^2$. Curves show the projections of the fit results for the continuum plus $b \rightarrow c$ background component (dot-dashed), total background without and with the $K_2^*(1430)^+\gamma$ component (dotted and dashed, respectively), $K_1(1270)^+\gamma$ (thin solid line) and $K_1(1400)^+\gamma$ (hatched) components, and the sum of all components (thick solid line).

($3 \pm 3\%$) [17]]. The fit result is shown in Fig. 2. We find 102 ± 22 events for the $B^+ \rightarrow K_1(1270)^+\gamma$ component with a significance of 7.3σ , while we fix the yields of the $K^*\gamma$, other $b \rightarrow s\gamma$, and charmless background components to be 2.3, 10.2, and 2.0 events, respectively. Similarly, we select the events with the $K^+\pi^-$ mass in the K^{*0} mass region, $0.8 \text{ GeV}/c^2 < M_{K\pi} < 1.0 \text{ GeV}/c^2$, in order to enhance the $K_1(1400)$ component [$\mathcal{B}(K_1(1400) \rightarrow K^*\pi) = (94 \pm 6)\%$ being much larger than $\mathcal{B}(K_1(1270) \rightarrow K^*\pi) = (16 \pm 5)\%$ [17]]. We find 23 ± 26 events for the $B^+ \rightarrow K_1(1400)^+\gamma$ component. Since the $K_1(1400)^+\gamma$ component is not significant, we set a 90% confidence level upper limit on the signal yield, N_{90} , which is calculated from the relation $\int_0^{N_{90}} \mathcal{L}(n)dn = 0.9 \int_0^\infty \mathcal{L}(n)dn$, where $\mathcal{L}(n)$ is the likelihood function with the signal yield fixed at n .

The systematic uncertainty related to the fitting procedure includes the same contributions as for the $K^+\pi^+\pi^-$ fit. The sub-branching fractions for the $K_1(1270)$ and the branching fraction for the $K_2^*(1430)\gamma$ as well the uncertainties in these quantities are taken from Ref. [17] and included in the fitting procedure. We also assign the uncertainty due to incorrectly reconstructed signal events, which is determined from a MC study. The total unbinned fitting errors are 20% (32%) for the $B^+ \rightarrow K_1(1270)^+\gamma$ [$B^+ \rightarrow K_1(1400)^+\gamma$] mode.

The reconstruction efficiency is obtained from the signal MC samples. For the inclusive measurement, we calculate the efficiency using the $K_1(1270)^+\gamma$ and $K^+\pi^+\pi^-\gamma$ nonresonant MC samples, and weighting according to the measured ratio of yields in those modes [$K_1(1400)^+\gamma$ and $K_2^*(1430)^+\gamma$ contributions are neglected]. We assume the same ratio for the $B^0 \rightarrow K^0\pi^+\pi^-\gamma$ efficiency. We estimate the systematic errors due to photon detection (2.8%), tracking (1% per track), charged particle identification (0.5% per particle), K_S^0 reconstruction (4.5%) and the likelihood ratio and π^0/η veto (6.1% for $K^+\pi^+\pi^-\gamma$, 3.2% for $K^0\pi^+\pi^-\gamma$). The total efficiency error is 7.6% (6.6%) for the $B^+ \rightarrow K^+\pi^+\pi^-\gamma$ ($B^0 \rightarrow K^0\pi^+\pi^-\gamma$) mode.

Using the signal yield and efficiency we find

$$\mathcal{B}(B^+ \rightarrow K_1(1270)^+\gamma) = (4.3 \pm 0.9 \pm 0.9) \times 10^{-5}, \quad (1)$$

where the first (second) error is statistical (systematic) assuming that the production of B^+ and B^0 in $Y(4S)$ decays is equal. We also measure the inclusive branching fractions of $B \rightarrow K\pi^+\pi^-\gamma$ given in Table I. We find that $\mathcal{B}(B^+ \rightarrow K^+\pi^+\pi^-\gamma)$ is consistent with the previous measurement with a significantly improved error [18]; the neutral one is measured with a similar branching fraction.

Similarly, we perform an unbinned maximum likelihood fit to the $B^0 \rightarrow K^0\pi^+\pi^-\gamma$ candidates to decompose $K_1(1270)^0$ and $K_1(1400)^0$. Because of the limited statistics

TABLE I. Yields from fits, detection efficiencies, branching fractions with statistical and systematic errors, and significances. The $K_1(1270)$ and $K_1(1400)$ are reconstructed as $K\pi^+\pi^-$ states which come through their subdecay channels.

	Yield	Efficiency	Branching Fraction (\mathcal{B})	Significance
$B^+ \rightarrow K_1(1270)^+\gamma$	102 ± 22	$(1.56 \pm 0.12)\%$	$(4.3 \pm 0.9 \pm 0.9) \times 10^{-5}$	7.3σ
$B^0 \rightarrow K_1(1270)^0\gamma$	$15.0^{+10.1}_{-8.2}$	$(0.34 \pm 0.02)\%$	$< 5.8 \times 10^{-5}$...
$B^+ \rightarrow K_1(1400)^+\gamma$	23 ± 26	$(2.68 \pm 0.20)\%$	$< 1.5 \times 10^{-5}$...
$B^0 \rightarrow K_1(1400)^0\gamma$	$-7.8^{+16.3}_{-13.8}$	$(0.61 \pm 0.04)\%$	$< 1.2 \times 10^{-5}$...
$B^+ \rightarrow K^+\pi^+\pi^-\gamma$	318 ± 22	$(8.36 \pm 0.64)\%$	$(2.50 \pm 0.18 \pm 0.22) \times 10^{-5}$	16σ
$B^0 \rightarrow K^0\pi^+\pi^-\gamma$	67 ± 10	$(1.82 \pm 0.12)\%$	$(2.4 \pm 0.4 \pm 0.3) \times 10^{-5}$	8.3σ

we do not obtain a significant result and set only upper limits.

To conclude, we observe a new radiative decay mode, $B^+ \rightarrow K_1(1270)^+\gamma$, with a branching fraction of $(4.3 \pm 0.9(\text{stat.}) \pm 0.9(\text{syst.})) \times 10^{-5}$, which is larger than theory predictions ($0.5 \sim 2.0$) $\times 10^{-5}$ [3,4]. The rates for $B \rightarrow K_1(1270)\gamma$ and $B \rightarrow K_1(1400)\gamma$ are sensitive to the magnitude and sign of the $K_1(1270) - K_1(1400)$ mixing angle. The large rate for $B^+ \rightarrow K_1(1270)^+\gamma$ compared to $B^+ \rightarrow K_1(1400)^+\gamma$ may be explained by a positive mixing angle [4]. This measurement of $B \rightarrow K_1(1270)\gamma$ shows that in the future it will be possible to determine the photon helicity using $B \rightarrow K_1\gamma$, $K_1 \rightarrow K\pi\pi$ and that time-dependent CP violation using $B^0 \rightarrow K_1(1270)^0\gamma$, $K_1(1270)^0 \rightarrow K_S^0\rho^0$ decays can also be studied. We also measure similar branching fractions for the inclusive decays $B^+ \rightarrow K^+\pi^+\pi^-\gamma$ and $B^0 \rightarrow K^0\pi^+\pi^-\gamma$. The latter is measured for the first time.

We thank the KEKB group for the excellent operation of the accelerator, the KEK Cryogenics group for the efficient operation of the solenoid, and the KEK computer group and the NII for valuable computing and Super-SINET network support. We acknowledge support from MEXT and JSPS (Japan); ARC and DEST (Australia); NSFC (Contract No. 10175071, China); DST (India); the BK21 program of MOEHRD and the CHEP SRC program of KOSEF (Korea); KBN (Contract No. 2P03B 01324, Poland); MIST (Russia); MESS (Slovenia); NSC and MOE (Taiwan); and DOE (USA).

*On leave from Nova Gorica Polytechnic, Nova Gorica.

- [1] CLEO Collaboration, R. Ammar *et al.*, Phys. Rev. Lett. **71**, 674 (1993).
 [2] We use K^* to denote $K^*(892)$ throughout the Letter.

- [3] S. Veseli and M. G. Olsson, Phys. Lett. B **367**, 309 (1996); D. Ebert, R. N. Faustov, V. O. Galkin, and H. Toki, Phys. Rev. D **64**, 054001 (2001); A. Safir, Eur. Phys. J. direct C **3**, 15 (2001).
 [4] H. Y. Cheng and C. K. Chua, Phys. Rev. D **69**, 094007 (2004).
 [5] M. Gronau, Y. Grossman, D. Pirjol, and A. Ryd, Phys. Rev. Lett. **88**, 051802 (2002).
 [6] D. Atwood, M. Gronau, and A. Soni, Phys. Rev. Lett. **79**, 185 (1997).
 [7] The inclusion of charge conjugate modes is implied unless otherwise stated, and K denotes both K^+ and K_S^0 throughout the Letter.
 [8] S. Kurokawa and E. Kikutani, Nucl. Instrum. Methods Phys. Res., Sect. A **499**, 1 (2003), and other papers included in this volume.
 [9] Belle Collaboration, A. Abashian *et al.*, Nucl. Instrum. Methods Phys. Res., Sect. A **479**, 117 (2002).
 [10] Variables with an asterisk are calculated in the c.m. frame.
 [11] R. A. Fisher, Annals of Eugenics **7**, 179 (1936).
 [12] Belle Collaboration, S. H. Lee *et al.*, Phys. Rev. Lett. **91**, 261801 (2003).
 [13] G. C. Fox and S. Wolfram, Phys. Rev. Lett. **41**, 1581 (1978).
 [14] ARGUS Collaboration, H. Albrecht *et al.*, Phys. Lett. B **229**, 304 (1989); $f(M) = A\{M\sqrt{1 - \frac{M^2}{E_{\text{beam}}^2}}\} \times \exp[-a(1 - \frac{M}{E_{\text{beam}}})]$, where A and a are free parameters.
 [15] Heavy Flavor Averaging Group, <http://www.slac.stanford.edu/xorg/hfag>.
 [16] Belle Collaboration, K. Abe *et al.*, Report No. BELLE-CONF-0348, contribution to the 2003 Lepton Photon conference.
 [17] Particle Data Group, S. Eidelman *et al.*, Phys. Lett. B **592**, 1 (2004).
 [18] CLEO Collaboration, T. E. Coan *et al.*, Phys. Rev. Lett. **84**, 5283 (2000); Belle Collaboration, S. Nishida *et al.*, Phys. Rev. Lett. **89**, 231801 (2002).